GEOPHYSICS, VOL. 74, NO. 5 (SEPTEMBER-OCTOBER 2009); P. WB177–WB191, 13 FIGS., 1 TABLE.
10.1190/1.3148439

Role of the inhomogeneity angle in anisotropic attenuation analysis

Jyoti Behura[1] and Ilya Tsvankin[2]

ABSTRACT

The inhomogeneity angle (the angle between the real and imaginary parts of the wave vector) is seldom taken into account in estimating attenuation coefficients from seismic data. Wave propagation through the subsurface, however, can result in relatively large inhomogeneity angles ξ, especially for models with significant attenuation contrasts across layer boundaries. Here we study the influence of the angle ξ on phase and group attenuation in arbitrarily anisotropic media using the first-order perturbation theory verified by exact numerical modeling. Application of the spectral-ratio method to transmitted or reflected waves yields the normalized group attenuation coefficient $\mathcal{A}_g$, which is responsible for amplitude decay along seismic rays. Our analytic solutions show that for a wide range of inhomogeneity angles, the coefficient $\mathcal{A}_g$ is close to the normalized *phase* attenuation coefficient $\mathcal{A}$ computed for $\xi = 0°$ ($\mathcal{A}|_{\xi=0°}$). The coefficient $\mathcal{A}|_{\xi=0°}$ can be inverted directly for the attenuation-anisotropy parameters, so no knowledge of the inhomogeneity angle is required for attenuation analysis of seismic data. This conclusion remains valid even for uncommonly high attenuation with the quality factor Q less than 10 and strong velocity and attenuation anisotropy. However, the relationship between group and phase attenuation coefficients becomes more complicated for relatively large inhomogeneity angles approaching so-called "forbidden directions." We also demonstrate that the velocity function remains practically independent of attenuation for a wide range of small and moderate angles ξ. In principle, estimation of the attenuation-anisotropy parameters from the coefficient $\mathcal{A}|_{\xi=0°}$ requires computation of the phase angle, which depends on the anisotropic velocity field. For moderately anisotropic models, however, the difference between the phase and group directions should not significantly distort the results of attenuation analysis.

INTRODUCTION

In attenuative media, the direction of maximum attenuation of a plane wave can differ from the propagation direction. This implies that the real part of wave vector $\mathbf{k}^R$ (propagation vector) deviates from the imaginary part $\mathbf{k}^I$ (attenuation vector), as illustrated in Figure 1. The angle between the vectors $\mathbf{k}^R$ and $\mathbf{k}^I$ is called the inhomogeneity angle, denoted here by ξ. When $\xi = 0°$, the plane wave is often characterized as "homogeneous;" when $\xi \neq 0°$, it is called "inhomogeneous." For plane-wave propagation, ξ represents a free parameter except for certain "forbidden directions" (Krebes and Le, 1994; Carcione and Cavallini, 1995; Červený and Pšenčík, 2005a, b), where solutions of the wave equation do not exist. If the wavefield is excited by a point source, the inhomogeneity angle is determined by the medium properties, including the boundary conditions (Zhu, 2006; Vavryčuk, 2007).

Alternatively, the wave vector in attenuative media can be parameterized in terms of the inhomogeneity parameter D (Boulanger and Hayes, 1993; Declercq et al., 2005; Červený and Pšenčík, 2005a):

$$\mathbf{k} = \omega(\sigma \mathbf{n} + i D \mathbf{m}), \tag{1}$$

such that

$$\mathbf{m} \cdot \mathbf{n} = 0, \tag{2}$$

where D is real, whereas σ is complex. The vector $\mathbf{n}$ specifies the direction of wave propagation and the vector $\mathbf{m}$ is orthogonal to it. The main advantage of this parameterization is that it eliminates forbidden directions from the solutions of the Christoffel equation (Červený and Pšenčík, 2005a).

Many results on attenuation analysis are obtained under the assumption that the inhomogeneity angle can be ignored (Hauge, 1981; Dasgupta and Clark, 1998; Zhu et al., 2007). For point-source radiation in homogeneous media, the influence of the inhomogene-

Manuscript received by the Editor 19 November 2008; revised manuscript received 6 February 2009; published online 28 September 2009.
[1]Formerly Colorado School of Mines, Department of Geophysics, Center for Wave Phenomena, Golden, Colorado, U.S.A.; presently BP America, Exploration and Production Technology, Houston, Texas, U.S.A. Email: jyoti.behura@bp.com; jbehura@dix.mines.edu.
[2]Colorado School of Mines, Department of Geophysics, Center for Wave Phenomena, Golden, Colorado, U.S.A. E-mail: ilya@dix.mines.edu.

ity angle is indeed small, unless the medium is anomalously attenuative and anisotropic (Zhu, 2006; Vavryčuk, 2007).

During wave propagation in layered media, however, the angle ξ can attain significant values. For the model in Figure 2, the wave vector in the elastic cap rock is real, whereas that in the attenuative reservoir is complex. Because the projections of the incident (real) and transmitted (complex) wave vectors onto the interface must be the same according to Snell's law, the imaginary part $\mathbf{k}^I$ of the wave vector in the reservoir is orthogonal to the interface. This implies that the inhomogeneity angle of the transmitted wave is equal to the transmission angle, which can reach 90°. It is also clear that the inhomogeneity angle of the wave reflected from the base of the reservoir can be large as well. This situation, for example, is always encountered in soft absorbing sediments beneath the ocean bottom.

Existing measurements of the inhomogeneity angle are limited to laboratory studies (Deschamps and Assouline, 2000; Huang et al., 1994). Indeed, although the angle ξ can be significant, its estimation from seismic data is extremely difficult. It seems natural to expect that the inhomogeneity angle should influence attenuation along the raypath (group attenuation), which is the only relevant attenuation measurement in seismic processing.

Attenuation analysis becomes particularly involved in anisotropic media where the ray might deviate significantly from both the phase direction and the direction of maximum attenuation. When the medium is anisotropic, the relationship between the angle ξ and the attenuation coefficients is obscured by the complexity of the exact equations. It can be inferred from the results of Gajewski and Pšenčík (1992) that in weakly attenuative media, the group attenuation coefficient yields the quality factor of the medium. Numerical modeling by Deschamps and Assouline (2000) also shows that group attenuation reflects the intrinsic viscoelasticity of the material. The analytic results of Vavryčuk (2008) and Červený and Pšenčík (2008a) indicate that group attenuation is insensitive to the inhomogeneity parameter. However, their asymptotic analysis is valid only for weak attenuation and plane waves with small values of the inhomogeneity parameter D.

Here we use first-order perturbation theory to study the influence of the inhomogeneity angle on group and phase attenuation coefficients. By perturbing an isotropic attenuative background, we obtain a weakly anisotropic medium with angular dependence of both velocity and attenuation. In contrast to the methodology of Červený and Pšenčík (2008a) and Vavryčuk (2008), our approach allows for arbitrarily large attenuation and strongly inhomogeneous waves. Therefore, this perturbation scheme helps us analyze wave propagation for a wide range of angles ξ including the vicinity of forbidden directions. First, we develop closed-form linearized expressions for group and phase attenuation in arbitrarily anisotropic media, which provide useful physical insight into the influence of the angle ξ. Then the general equations are simplified for the special case of TI media by expressing them through Thomsen-style anisotropy parameters. Finally, we corroborate the conclusions drawn from the analytic expressions by exact numerical modeling.

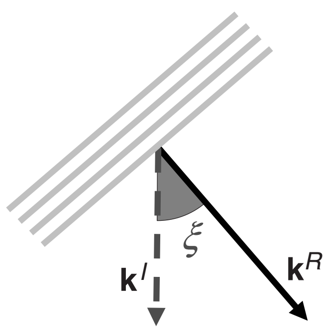

Figure 1. Plane wave with a nonzero inhomogeneity angle ξ. The wave propagates in the direction $\mathbf{k}^R$ (perpendicular to the planes of constant phase) and attenuates most rapidly in the direction $\mathbf{k}^I$.

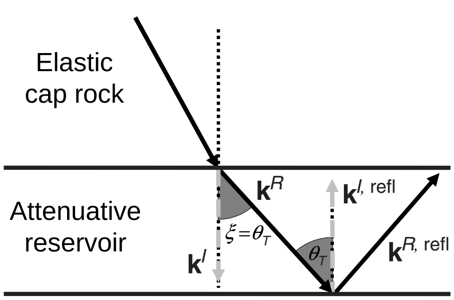

Figure 2. Illustration of the reflection/transmission problem at the interface between a purely elastic cap rock and an attenuative reservoir. The real and imaginary parts of the wave vector of the transmitted wave are $\mathbf{k}^R$ and $\mathbf{k}^I$, and $\mathbf{k}^{R,\mathrm{refl}}$ and $\mathbf{k}^{I,\mathrm{refl}}$ correspond to the reflected wave. As discussed in the text, the inhomogeneity angle ξ of the transmitted wave is equal to transmission angle θ_T.

PHASE AND GROUP ATTENUATION COEFFICIENTS

The Christoffel equation, which describes plane-wave propagation in anisotropic media, can be solved for the real (k^R) and imaginary (k^I) parts of the wave vector. The ratio k^I/k^R yields the phase attenuation per wavelength, which is called the normalized phase-attenuation coefficient $\mathcal{A}$ (Zhu and Tsvankin, 2006):

$$\mathcal{A} = \frac{k^I}{k^R}. \tag{3}$$

For a nonzero inhomogeneity angle ξ, the coefficient $\mathcal{A}$ is a measure of attenuation along the vector $\mathbf{k}^I$ rather than $\mathbf{k}^R$. Also, in seismic data processing, attenuation is measured along the raypath, which deviates from the phase direction $\mathbf{k}^R$ when the medium is anisotropic.

Typically, attenuation is computed from seismic data using the spectral-ratio method (e.g., Johnston and Toksöz, 1981; Tonn, 1991), which has been extended to anisotropic media (Zhu et al., 2007). If two receivers record the same event at two different locations along a raypath, the attenuation coefficient can be estimated from the ratio S of the measured amplitude spectra:

$$\ln S = \ln \mathcal{G} - k_g^I\, l, \tag{4}$$

where $\mathcal{G}$ contains the reflection/transmission coefficients, source/receiver radiation patterns, and geometrical spreading along the raypath, k_g^I is the average group attenuation coefficient, and l is the distance between the two receivers. Assuming that the medium between the receivers is homogeneous, equation 4 can be rewritten in terms of the group velocity V_g and traveltime t:

$$\ln S = \ln \mathcal{G} - k_g^I V_g t, \\ = \ln \mathcal{G} - \omega \mathcal{A}_g t, \tag{5}$$

where ω is the angular frequency and $\mathcal{A}_g = k_g^I / k_g^R = k_g^I / (\omega / V_g)$ is the normalized group attenuation coefficient. It follows from equation 5 that by estimating the slope of $\ln S$ expressed as a function of ω, we can compute the group attenuation along the raypath, if the traveltime t is known. Therefore, $\mathcal{A}_g$ is the measure of attenuation obtained from seismic data.

If the medium is anisotropic (or isotropic, but the inhomogeneity angle is large, as discussed below), the group-velocity vector $\mathbf{V}_g$ deviates from the phase direction parallel to $\mathbf{k}^R$. To simplify the analytic development, we choose a coordinate frame in which $\mathbf{k}^R$ coincides with the axis x_3 and $\mathbf{k}^I$ is confined to the $[x_1, x_3]$-plane (Figure 3). The group attenuation coefficient k_g^I can be found by projecting the phase attenuation vector $\mathbf{k}^I$ onto the group direction:

$$k_g^I = \frac{1}{V_g} (\mathbf{k}^I \cdot \mathbf{V}_g), \tag{6}$$

$$= k^I (\cos \xi \cos \psi + \sin \xi \sin \psi \cos \phi), \tag{7}$$

where ψ is the angle between $\mathbf{k}^R$ and $\mathbf{V}_g$ (group angle) and ϕ is the azimuth of $\mathbf{V}_g$ with respect to the $[x_1, x_3]$-plane (Figure 3). For isotropic media and symmetry planes in anisotropic media, $\mathbf{V}_g$ lies in the plane formed by vectors $\mathbf{k}^R$ and $\mathbf{k}^I$ (i.e., $\phi = 0$), and k_g^I is given by

$$k_g^I = k^I \cos(\xi - \psi). \tag{8}$$

Using equation 7, the normalized group attenuation coefficient $\mathcal{A}_g$ can be represented as

$$\mathcal{A}_g = \frac{k_g^I}{k_g^R} = \frac{k^I \cos \xi \cos \psi \, (1 + \tan \xi \tan \psi \cos \phi)}{\omega / V_g}. \tag{9}$$

The group velocity can be obtained from the well-known relation (e.g., Červený and Pšenčík, 2006)

$$\frac{1}{\omega} \mathbf{k}^R \cdot \mathbf{V}_g = 1, \tag{10}$$

or

$$\frac{\omega}{V_g} = k^R \cos \psi. \tag{11}$$

Substituting equation 11 into equation 9 yields

$$\mathcal{A}_g = \frac{k^I}{k^R} \cos \xi \, (1 + \tan \xi \tan \psi \cos \phi). \tag{12}$$

Equation 12 can be used to compute the exact coefficient $\mathcal{A}_g$ for arbitrarily anisotropic, attenuative media and any angle ξ. If the group-velocity vector is confined to the plane formed by $\mathbf{k}^R$ and $\mathbf{k}^I$ (see above), $\cos \phi = 1$ and equation 12 becomes

$$\mathcal{A}_g = \frac{k^I}{k^R} \frac{\cos(\xi - \psi)}{\cos \psi}. \tag{13}$$

For a zero inhomogeneity angle, the coefficient $\mathcal{A}_g$ reduces to

$$\mathcal{A}_g(\xi = 0^\circ) = \left. \frac{k^I}{k^R} \right|_{\xi = 0^\circ} = \mathcal{A}|_{\xi = 0^\circ}. \tag{14}$$

Equation 14 demonstrates that even for arbitrary anisotropy, the group attenuation coefficient coincides with the phase attenuation coefficient computed for $\xi = 0^\circ$ (Zhu, 2006). However, it is unclear how $\mathcal{A}_g$ is related to phase attenuation for a nonzero ξ and what role is played by the inhomogeneity angle in the estimation of the attenuation coefficient.

ISOTROPIC MEDIA

To evaluate the influence of the inhomogeneity angle on velocity and attenuation in isotropic media, we obtain the real and imaginary parts of the vector $\mathbf{k}$ from the wave equation. The derivation, discussed in Appendix A, shows that the solution exists only if $\mathbf{k}^R \cdot \mathbf{k}^I > 0$, which means that the inhomogeneity angle in isotropic media should be smaller than 90° (we assume that $\xi > 0^\circ$ because positive and negative inhomogeneity angles are equivalent in the absence of anisotropy). Therefore, the attenuation vector $\mathbf{k}^I$ cannot deviate from $\mathbf{k}^R$ by 90° or more, and angles $\xi \geq 90^\circ$ correspond to forbidden directions. Note that for isotropic *nonattenuative* media, the inhomogeneity angle of an evanescent (inhomogeneous) plane wave is always equal to 90°, which explains the properties of surface and nongeometric modes (Tsvankin, 2005).

The squared magnitudes of the vectors $\mathbf{k}^R$ and $\mathbf{k}^I$ for $\xi < 90^\circ$ (Appendix A) are given by

$$(k^R)^2 = \frac{\omega^2}{2V^2} \left[\sqrt{1 + \frac{1}{(Q \cos \xi)^2}} + 1 \right], \tag{15}$$

and

$$(k^I)^2 = \frac{\omega^2}{2V^2} \left[\sqrt{1 + \frac{1}{(Q \cos \xi)^2}} - 1 \right], \tag{16}$$

where $V = \sqrt{a_{33}^R}$ is the real part of the medium velocity and a_{ij} is the density-normalized stiffness tensor. The only approximation used to derive equations 15 and 16 is that quadratic and higher-order terms in the inverse quality factor $1/Q$ (but not in $1/(Q \cos \xi)$) can be ne-

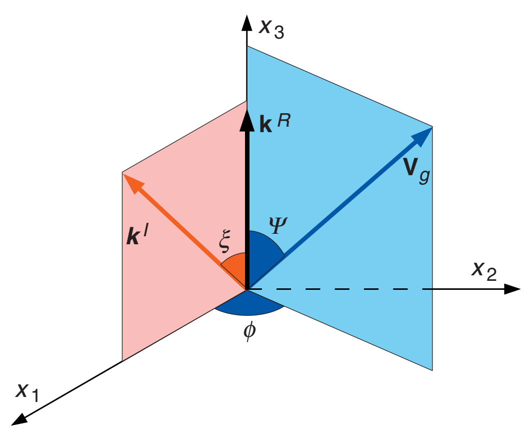

Figure 3. Plane wave propagating along the coordinate axis x_3 in an anisotropic attenuative medium. The group angle ψ is the deviation of the group-velocity vector $\mathbf{V}_g$ from the real part $\mathbf{k}^R$ of the wave vector. The azimuth of the vector $\mathbf{V}_g$ with respect to the plane formed by $\mathbf{k}^R$ and $\mathbf{k}^I$ is denoted by ϕ.

glected compared to unity. Equivalent solutions for k^R and k^I in isotropic media are given in Červený and Pšenčík (2005a).

Small and moderate inhomogeneity angles

The dependence of the wave vector on the inhomogeneity angle is controlled by the product $(Q\cos\xi)$. If the angle ξ is not close to 90° and the medium does not have uncommonly strong attenuation, we can assume that $(Q\cos\xi)\gg 1$ and simplify equations 15 and 16 to (see Appendix A)

$$k^R = \frac{\omega}{V}, \tag{17}$$

$$k^I = \frac{\omega}{2VQ\cos\xi}. \tag{18}$$

According to equation 17, for $(Q\cos\xi)\gg 1$ the velocity of wave propagation is equal to V and is independent of the inhomogeneity angle and of attenuation. Using equations 17 and 18, we find the normalized phase attenuation coefficient $\mathcal{A}$ as

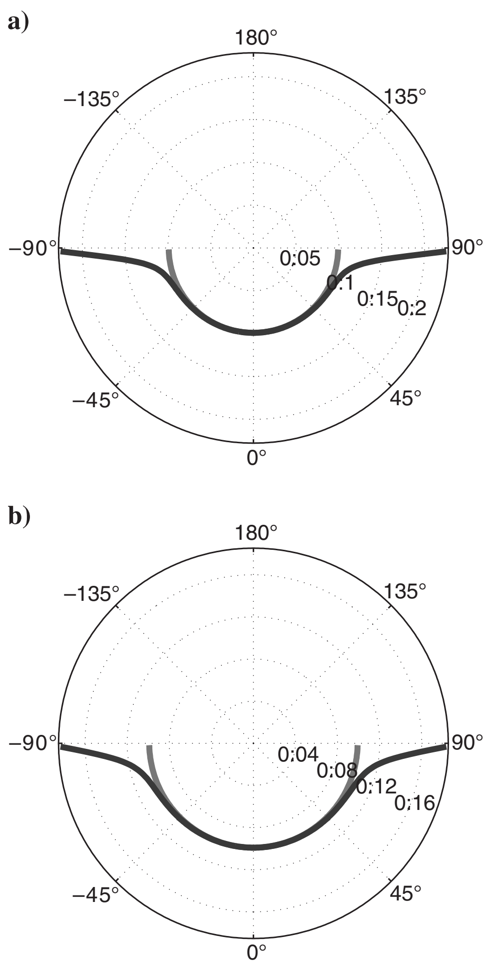

Figure 4. Exact (a) P-wave and (b) S-wave coefficient $\mathcal{A}|_{\xi=0^\circ}$ (equation 3, gray curve) and the normalized group attenuation $\mathcal{A}_g$ (equation 12, black curve) in isotropic media as a function of the inhomogeneity angle ξ (numbers on the perimeter). The quality factors are $Q_P = Q_S = 5$.

$$\mathcal{A} = \frac{k^I}{k^R} = \frac{1}{2Q\cos\xi}. \tag{19}$$

In general, the inhomogeneity angle also changes the group velocity and group angle. For $(Q\cos\xi)\gg 1$, however, the influence of ξ is negligible (Appendix A):

$$\tan\psi = \frac{\tan\xi}{1+2Q^2} \ll 1, \tag{20}$$

and $V_g \approx V$. The normalized group attenuation coefficient $\mathcal{A}_g$ (equation 12) then becomes

$$\mathcal{A}_g = \frac{k^I\cos\xi}{k^R}. \tag{21}$$

If the wave vector is described by equations 17 and 18, equation 21 yields

$$\mathcal{A}_g = \frac{1}{2Q} = \mathcal{A}|_{\xi=0^\circ}. \tag{22}$$

Therefore, for a wide range of common inhomogeneity angles, the group attenuation coefficient $\mathcal{A}_g$ does not depend on the angle ξ and is close to the phase attenuation coefficient $\mathcal{A}$ computed for $\xi = 0°$. Later we demonstrate that this result remains valid for much more complicated models with anisotropic velocity and attenuation functions. Equation 22 also shows that seismic attenuation measurements (i.e., the coefficient $\mathcal{A}_g$) for isotropic media provide a direct estimate of the quality factor Q. This conclusion applies to both P- and S-waves and a wide range of angles ξ (Figure 4).

Large inhomogeneity angles

For large inhomogeneity angles approaching 90°, the assumption $(Q\cos\xi)\gg 1$, used to derive equations 17 and 18, is no longer satisfied. In the limit of $(Q\cos\xi)\ll 1$ ($\xi\to 90°$), equations 15 and 16 give completely different approximate solutions for the wave vector (Appendix A):

$$k^R = \frac{\omega}{V\sqrt{2Q\cos\xi}}\left(1+\frac{Q\cos\xi}{2}\right), \tag{23}$$

and

$$k^I = \frac{\omega}{V\sqrt{2Q\cos\xi}}\left(1-\frac{Q\cos\xi}{2}\right). \tag{24}$$

Dropping quadratic and higher-order terms in $(Q\cos\xi)$, we find

$$\mathcal{A} = \frac{k^I}{k^R} = 1 - Q\cos\xi. \tag{25}$$

The velocity of wave propagation, determined primarily by the denominator of the expression for k^R (equation 23), is proportional to $\sqrt{Q\cos\xi}$ and goes to zero when the inhomogeneity angle approaches 90°.

When $\xi\to 90°$, the influence of the inhomogeneity angle on the group quantities ψ, V_g, and $\mathcal{A}_g$ is no longer negligible. The group angle for large inhomogeneity angles becomes (see Appendix A)

$$\tan\psi = \frac{1}{Q} - \cos\xi. \quad (26)$$

Equation 26 demonstrates that for strong attenuation (small Q) the group-velocity vector deviates from the phase direction toward the attenuation vector when $\xi \to 90°$. Note that despite the medium being isotropic, the group and phase directions differ because of nonzero values of ξ.

The coefficient $\mathcal{A}_g$ for large angles ξ can be obtained by substituting equations 25 and 26 into equation 12:

$$\mathcal{A}_g = (1 - Q\cos\xi)\left[\cos\xi + \left(\frac{1}{Q} - \cos\xi\right)\sin\xi\right]. \quad (27)$$

Linearizing equation 27 in $\cos\xi$ yields

$$\mathcal{A}_g = \frac{1}{Q} - \cos\xi. \quad (28)$$

Equation 28 shows that the group attenuation coefficient $\mathcal{A}_g$ for large inhomogeneity angles reduces to just $\tan\psi$ (see equation 26). Therefore, whereas the real and imaginary parts of the wave vector (equations 23 and 24) become infinite as $\xi \to 90°$, the group attenuation coefficient approaches $1/Q$ and is about twice as large as $\mathcal{A}|_{\xi=0°}$ (Figure 4). Hence, for large angles ξ close to 90°, seismic attenuation measurements in isotropic media do not provide a direct estimate of the quality factor because $\mathcal{A}_g$ rapidly increases with ξ from and $1/(2Q)$ to $1/Q$.

Although the presence of anisotropy makes treatment of wave propagation in attenuative media much more complicated, several key conclusions drawn above prove to be valid for models with anisotropic velocity and attenuation functions.

ANISOTROPIC MEDIA

The dependence of attenuation on the inhomogeneity angle ξ in anisotropic media is influenced by the angular variation of the phase quantities and by the difference between the group and phase directions. Using the Christoffel equation B-1, the phase attenuation coefficient $\mathcal{A}$ can be computed for arbitrary values of the angle ξ. Then general group-velocity equations (e.g., Tsvankin, 2005) can be employed to obtain the group attenuation coefficient. It would be useful, however, to develop analytic expressions for phase and group attenuation that provide physical insight into the contribution of the inhomogeneity angle. To derive analytic expressions for $\mathbf{k}^R$, $\mathbf{k}^I$, and $\mathcal{A}_g$ in arbitrarily anisotropic media, we use first-order perturbation theory, as discussed in Appendix A. The analytic development is supported by numerical modeling based on exact solutions.

Perturbation of the complex wave vector

We consider an isotropic, attenuative background medium, which is perturbed to obtain anisotropic velocity and attenuation functions. The real and imaginary parts of the wave vector in the background are denoted by $\mathbf{k}^{R,0}$ and $\mathbf{k}^{I,0}$, respectively. We choose the coordinate frame in which $\mathbf{k}^{R,0}$ coincides with the x_3-axis and $\mathbf{k}^{I,0}$ lies in the $[x_1,x_3]$-plane. The angle ξ is kept fixed, so the real and imaginary parts of the perturbed wave vector $\mathbf{k} = \mathbf{k}^R - i\mathbf{k}^I$ remain parallel to the corresponding parts of the background vector $\mathbf{k}^0$.

First, we obtain linearized expressions for the perturbations Δk^R and Δk^I in arbitrarily anisotropic media using the coordinate frame defined by $\mathbf{k}^R$ and $\mathbf{k}^I$ (equations B-15–B-20 in Appendix B). To express Δk^R and Δk^I in a fixed coordinate frame, one has to rotate the perturbation density-normalized stiffness tensor Δa_{ijkl} accordingly. For example, to derive Δk^R and Δk^I for TI media as a function of the phase angle θ (the angle between $\mathbf{k}^R$ and the symmetry axis), the tensor Δa_{ijkl} in equations B-15–B-20 is rotated about the x_2-axis by the angle θ.

For the special case of P-wave propagation in TI media, the perturbations Δk^R and Δk^I take the form

$$\frac{\Delta k_{\mathrm{P}}^R}{k_{\mathrm{P}}^{R,0}} = -(\delta\sin^2\theta\cos^2\theta + \varepsilon\sin^4\theta) \quad (29)$$

and

$$\frac{\Delta k_{\mathrm{P}}^I}{k_{\mathrm{P}}^{I,0}} = \delta_Q\sin^2\theta\cos^2\theta + \varepsilon_Q\sin^4\theta - (\delta\sin^2\theta\cos^2\theta + \varepsilon\sin^4\theta) - [\delta + 2(\varepsilon - \delta)\sin^2\theta]\sin 2\theta\tan\xi, \quad (30)$$

where ε and δ are Thomsen velocity-anisotropy parameters, and ε_Q and δ_Q are Thomsen-style attenuation-anisotropy parameters (Zhu and Tsvankin, 2006). The parameter ε_Q determines the fractional difference between the P-wave phase attenuation coefficients $\mathcal{A}|_{\xi=0°}$ in the horizontal and vertical directions, and δ_Q controls the coefficient $\mathcal{A}|_{\xi=0°}$ in the vicinity of the symmetry axis. Equations 29 and 30 are derived for the attenuation vector $\mathbf{k}^I$ confined to the plane defined by $\mathbf{k}^R$ and the symmetry axis. Similar expressions for SV- and SH-waves in TI media are given in Appendix C (equations C-1–C-4).

Note that the real part Δk^R of the linearized perturbation in the wave vector in equations 29, C-1, and C-3 is independent of the inhomogeneity angle and is governed entirely by velocity anisotropy. This conclusion is corroborated by the numerical example in Figure 5. As the inhomogeneity angle varies from 0° to 70°, there is no noticeable change in k^R even in the presence of velocity anisotropy (Figure 5c and d) and attenuation anisotropy (Figure 5e and f). The "isotropic" behavior of k^R in Figure 5e and f indicates that attenuation anisotropy has little influence on the velocity function, which is controlled by the velocity-anisotropy parameters (Figure 5c and d). Whereas equations 29, C-1, and C-3 remain accurate for a wide range of ξ (Figure 5b, d, and f) and strong attenuation anisotropy, they break down for the angle ξ approaching 90°.

The attenuation vector k^I (equations 30, C-2, and C-4), on the other hand, is influenced by both velocity and attenuation anisotropy, as well as by the inhomogeneity angle ξ. The increase in ξ from 0° to 70° in Figure 6 causes a substantial change in k^I, both for isotropic and TI media. Figure 6d-i illustrates the dependence of k^I on the velocity- and attenuation-anisotropy parameters. It is interesting to note that for small ξ, the contribution of velocity and attenuation anisotropy to k^I (equations 30, C-2, and C-4) is of the same order. With increasing ξ, however, the influence of velocity anisotropy (Figure 6f) becomes more pronounced compared to that of attenuation anisotropy (Figure 6i) because the $\tan\xi$-term in equation 30 depends just on ε and δ. Figure 6 also demonstrates that equation 30 deviates from the exact k^I only for large angles ξ, with the error controlled primarily by the velocity-anisotropy parameters.

Normalized group attenuation coefficient

As discussed above, for a zero inhomogeneity angle, the normalized group attenuation coefficient $\mathcal{A}_g$ coincides with $\mathcal{A}|_{\xi=0°}$ (equation 14). This conclusion, which is valid for all wave modes, is supported by Figure 7a and b, in which the coefficients $\mathcal{A}|_{\xi=0°}$ (gray curve) and $\mathcal{A}_g$ (black) practically coincide when $\xi = 0°$.

To examine the influence of the angle ξ on $\mathcal{A}_g$, we linearize equation 12 in terms of perturbations of the wave vector:

$$\mathcal{A}_g = \frac{k^{I,0} + \Delta k^I}{k^{R,0} + \Delta k^R} \cos\xi (1 + \tan\xi \tan\psi \cos\phi)$$
$$= \frac{k^{I,0}}{k^{R,0}} \left(1 + \frac{\Delta k^I}{k^{I,0}} - \frac{\Delta k^R}{k^{R,0}}\right) \cos\xi (1 + \tan\xi \tan\psi \cos\phi). \quad (31)$$

Taking into account that $k^{I,0}/k^{R,0} = 1/(2Q^0 \cos\xi)$ (equation 19), we find

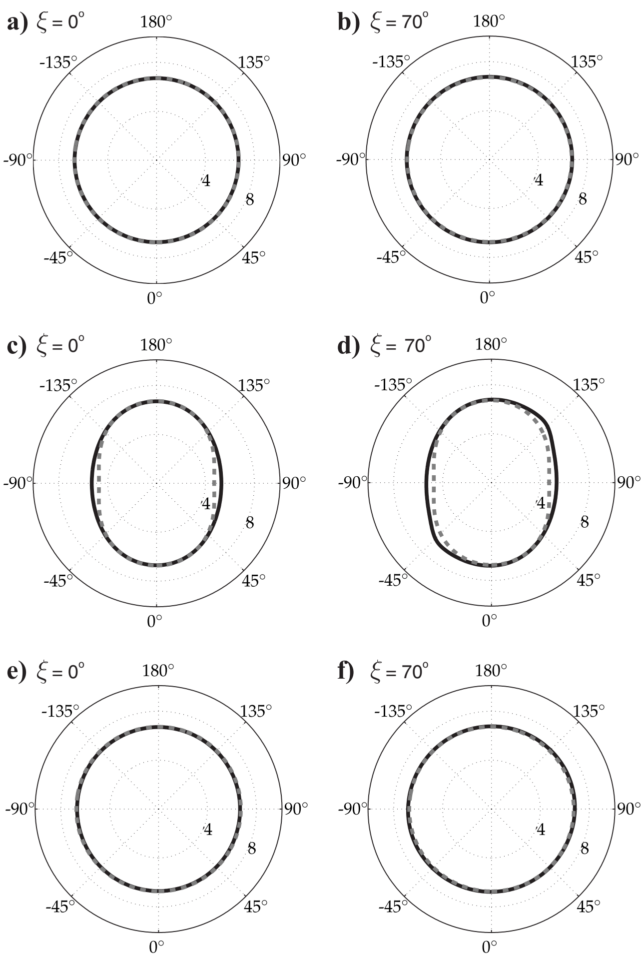

Figure 5. Exact real part k^R (in 100 m^{-1}) of the P-wave vector $\mathbf{k}$ (solid lines) and approximate $k^R = k^{R,0} + \Delta k^R$ from equation 29 (dashed lines) for (a), (c), and (e) $\xi = 0°$ and (b), (d), and (f) $\xi = 70°$ as a function of the phase angle (numbers on the perimeter). The model in (a) and (b) is isotropic; in (c) and (d) it is anisotropic in terms of velocity but has isotropic attenuation; and in (e) and (f) it has isotropic velocity and anisotropic attenuation (Table 1). The frequency is 30 Hz.

$$\mathcal{A}_g = \frac{1}{2Q^0} \left(1 + \frac{\Delta k^I}{k^{I,0}} - \frac{\Delta k^R}{k^{R,0}}\right)(1 + \tan\xi \tan\psi \cos\phi). \quad (32)$$

Equation 32 is valid in arbitrarily anisotropic media for all wave modes. Substituting equations B-15 and B-16 for Δk^R and Δk^I and equation B-26 for the product $\tan\psi \cos\phi$ into equation 32, we obtain the group attenuation coefficient for P-waves linearized in Δa_{ij}:

$$\mathcal{A}_{g,\mathrm{P}} = \frac{1}{2Q_{\mathrm{P0}}} - \frac{1}{2V_{\mathrm{P0}}^2} \left(\frac{\Delta a_{33}^R}{Q_{\mathrm{P0}}} - \Delta a_{33}^I\right), \quad (33)$$

where Q_{P0} and V_{P0} are the P-wave quality factor and velocity, respectively, in the background. Similar expressions for S_1- and S_2-waves are given in Appendix B (equations B-30 and B-31).

Below, we analyze equation 33 for the special case of P-wave propagation in TI media with arbitrary symmetry-axis orientation. As mentioned earlier, to express $\mathcal{A}_g$ through the phase angle θ with the symmetry axis, the tensor Δa_{ijkl} in equation 33 has to be rotated around the x_2-axis. Then we linearize $\mathcal{A}_g$ in the velocity- and attenuation-anisotropy parameters to obtain

$$\mathcal{A}_{g,\mathrm{P}} = \frac{1}{2Q_{\mathrm{P0}}} (1 + \delta_Q \sin^2\theta \cos^2\theta + \varepsilon_Q \sin^4\theta). \quad (34)$$

Similar approximate expressions for the group attenuation coefficient of SV- and SH-waves are given in Appendix C (equations C-10 and C-11).

Therefore, the inhomogeneity angle has no influence on the approximate group attenuation coefficient. Furthermore, as discussed below, $\mathcal{A}_{g,\mathrm{P}}$ in equation 34 coincides with the linearized P-wave

Table 1. Medium parameters used in the numerical tests. For all models, the P- and S-wave symmetry-direction velocities (V_{P0} and V_{S0}) are 2800 m/s and 1700 m/s, respectively.

Figure	ξ	ε	δ	γ	Q_{P0}	Q_{S0}	ε_Q	δ_Q	γ_Q
5a, b	0°, 70°	0	0	0	10	10	0	0	0
5c, d	0°, 70°	0.3	0.2	0	10	10	0	0	0
5e, f	0°, 70°	0	0	0	10	10	0.6	0.4	0
6a, b, c	0°, 45°, 70°	Same as in Figure 5a and b							
6d, e, f	0°, 45°, 70°	Same as in Figure 5c and d							
6g, h, i	0°, 45°, 70°	Same as in Figure 5e and f							
7a	0°	0.3	0.2	0	10	10	0.6	0.4	0
7b	0°	0	0	0.3	10	10	0	0	0.5
8	—	0.3	0.2	0	5	5	0.6	0.4	0
9a	60°	0	0	0	10	10	0	0	0
9b	60°	0.3	0.2	0	10	10	0	0	0
9c	60°	0.6	0.4	0	10	10	0	0	0
9d	60°	0	0	0	10	10	0.6	0.4	0
10a, b	60°	0.6	0.4	0	10	10	0.6	0.4	0
10c, d	60°	0	0	0.5	10	10	0	0	0.5
11	—	0	0	0.3	5	5	0	0	0.5
12a	—	0	0	1	5	5	0	0	−0.5
12b	—	0	0	0.3	5	5	0	0	−0.5

phase attenuation coefficient for a zero inhomogeneity angle ($\mathcal{A}|_{\xi=0^\circ}$) derived by Zhu and Tsvankin (2006). Equation 34 noticeably deviates from the exact $\mathcal{A}_g$ only when the angle ξ approaches forbidden directions (Figure 8); the behavior of $\mathcal{A}_g$ for large inhomogeneity angles is analyzed in more detail below.

Note that the linearized $\mathcal{A}_g$ (equations 34, C-10, and C-11) is controlled by attenuation anisotropy and does not depend on velocity-anisotropy parameters. This conclusion is confirmed by the exact modeling results in Figure 9a and b, where the coefficient $\mathcal{A}_g$ remains insensitive even to strong velocity anisotropy with $\varepsilon = 0.6$ and $\delta = 0.4$ when $\xi = 60^\circ$ (Figure 9c). The presence of attenuation anisotropy, on the other hand, results in a substantial change in $\mathcal{A}_g$ (Figure 9d).

Relationship between group and phase attenuation

The normalized phase attenuation coefficient $\mathcal{A}|_{\xi=0^\circ}$ can be obtained from the Christoffel equation and expressed through attenuation-anisotropy parameters (Zhu and Tsvankin, 2006). As shown above, the coefficient $\mathcal{A}_g$ coincides with $\mathcal{A}|_{\xi=0^\circ}$ for a wide range of ξ in isotropic media and for $\xi = 0^\circ$ in anisotropic media (equation 14).

Using perturbation analysis, we obtained closed-form expressions for coefficient $\mathcal{A}|_{\xi=0^\circ}$ in arbitrarily anisotropic media linearized in Δa_{ij} (Appendix B). For P-waves,

$$\mathcal{A}|_{\xi=0^\circ,\mathrm{P}} = \frac{1}{2Q_{\mathrm{P0}}} - \frac{1}{2V_{\mathrm{P0}}^2}\left(\frac{\Delta a_{33}^R}{Q_{\mathrm{P0}}} - \Delta a_{33}^I\right). \tag{35}$$

Similar expressions for S_1- and S_2-waves are given in Appendix B. Comparison of equations 33 and 35 shows that for a wide range of angles ξ (except for values close to 90°; see below), the linearized coefficient $\mathcal{A}_g$ coincides with $\mathcal{A}|_{\xi=0^\circ}$. This conclusion is also valid for S_1- and S_2-waves (compare equations B-30 and B-31 with equations B-24 and B-25).

The approximate P-wave phase attenuation coefficient for TI media can be found as a simple function of attenuation-anisotropy parameters (Zhu and Tsvankin, 2006):

$$\mathcal{A}|_{\xi=0^\circ,\mathrm{P}} = \frac{1}{2Q_{\mathrm{P0}}}(1 + \delta_Q \sin^2\theta\cos^2\theta + \varepsilon_Q \sin^4\theta). \tag{36}$$

Zhu and Tsvankin (2006) also provide similar linearized expressions for SV- and SH-waves reproduced in Appendix B. As is the case for arbitrary ansisotropy, the coefficient $\mathcal{A}|_{\xi=0^\circ}$ in equation 36 coincides with $\mathcal{A}_g$ in equation 34.

Figure 10a and b demonstrate that the maximum difference between the exact coefficients $\mathcal{A}_g$ and $\mathcal{A}|_{\xi=0^\circ}$ does not exceed 10% even for strong attenuation ($Q_{33} = 10$) and uncommonly large anisotropy parameters ($\varepsilon = \varepsilon_Q = 0.6$ and $\delta = \delta_Q = 0.4$). The coefficients $\mathcal{A}_g$ and $\mathcal{A}|_{\xi=0^\circ}$ also are close for SV- and SH-waves, which confirms the analytic results of Appendix C (Figure 10c and d).

Group attenuation for large inhomogeneity angles

The above conclusions about the influence of the inhomogeneity angle on phase velocity and attenuation no longer hold for large inhomogeneity angles approaching forbidden directions. As shown above for isotropic media, when $(Q\cos\xi) \ll 1$, the group attenuation coefficient varies with the angle ξ and differs from $\mathcal{A}|_{\xi=0^\circ}$.

To study the influence of large ξ analytically, we follow the same perturbation-based approach (Appendix B) but with different background values of the wave vector, group velocity, and group angle (equations 23–26). For simplicity, here we analyze only the special case of elliptical anisotropy in TI media (i.e., SH-waves); more general solutions for shear waves in arbitrarily anisotropic media are given in Appendix D. Numerical tests demonstrate that our conclusions remain valid for all wave modes and any anisotropic symmetry.

According to equation D-6, the coefficient $\mathcal{A}_g$ for large inhomogeneity angles becomes a function of ξ and cannot serve as a measure of intrinsic attenuation. As is the case for isotropy, $\mathcal{A}_g$ in anisotropic

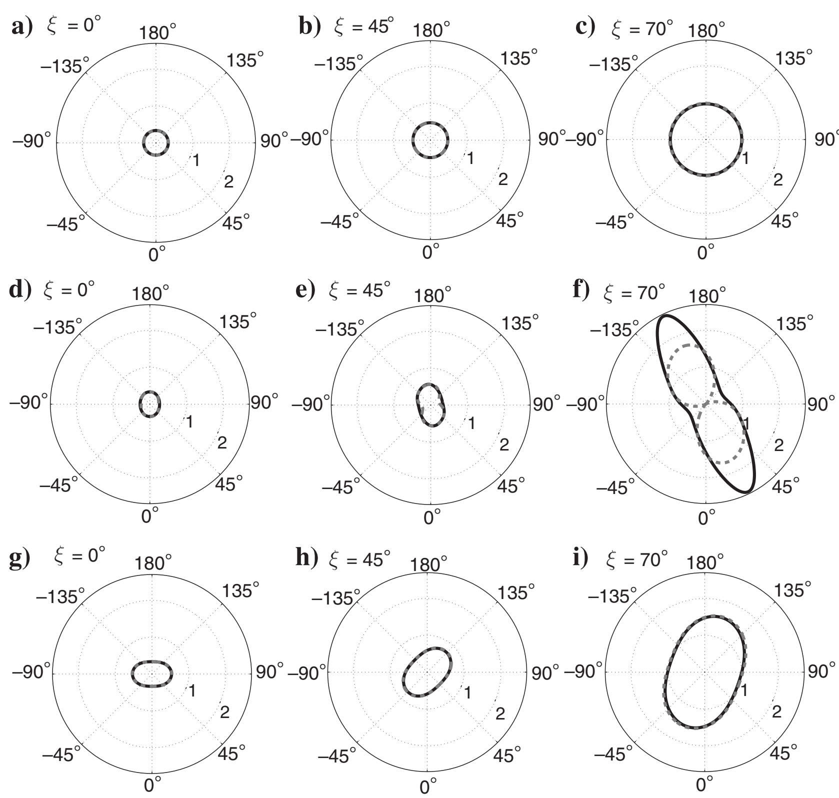

Figure 6. Exact imaginary part k^I of the P-wave vector $\mathbf{k}$ (solid lines) and approximate $k^I = k^{I,0} + \Delta k^I$ (in 100 m^{-1}) from equation 30 (dashed lines) for (a), (d), and (g) $\xi = 0^\circ$, (b), (e), and (h) $\xi = 45^\circ$, and (c), (f), and (i) $\xi = 70^\circ$ as a function of the angle between $\mathbf{k}^I$ and the symmetry axis. In (a), (b), and (c), both velocity and attenuation are isotropic; in (d), (e), and (f), only velocity varies with angle, whereas attenuation is isotropic; in (g), (h), and (i), attenuation varies with angle, whereas velocity is isotropic. The model parameters are given in Table 1. The frequency is 30 Hz.

media is always finite (and does not go to zero), even though the real and imaginary parts of the wave vector (equation D-3) become infinite.

When the medium is isotropic, a physical solution of the wave equation exists only for $-90° < \xi < 90°$ (equation A-5; also see Červený and Pšenčík, 2005a). The bounds for the inhomogeneity angle in arbitrarily anisotropic media depend on both velocity and attenuation anisotropy and can be derived from equation D-3 using the inequalities $k^R > 0$ and $k^I > 0$. For the special case of elliptical anisotropy (equation D-4), the inhomogeneity angle should satisfy

$$\cos\xi + \frac{\gamma \sin 2\theta}{2} \sin\xi > \frac{\gamma_Q \cos 2\theta}{4Q_{S0}}, \tag{37}$$

which yields the following bounds for ξ:

$$-\beta - \alpha < \xi < \beta - \alpha, \tag{38}$$

where

$$\alpha = \tan^{-1}\left(\frac{-\gamma \sin 2\theta}{2}\right) \tag{39}$$

and

$$\beta = \cos^{-1}\left(\frac{\gamma_Q \cos 2\theta}{4Q_{S0}}\right). \tag{40}$$

Equivalent expressions for the bounds on ξ for SH-wave propagation in the symmetry plane of a monoclinic medium are given by Červený and Pšenčík (2005a) in terms of the inhomogeneity parameter D.

For wave propagation along the symmetry axis or perpendicular to it ($\theta = 0°$ or $90°$), the angle $\alpha = 0°$ and the bounds on ξ are symmetric with respect to $\xi = 0°$ (equations 38 and 40; Figure 11). It is also clear from equation 40 that $\beta \approx 90°$ because the ratio γ_Q/Q_{S0} typically is small. Hence, for $\theta = 0°$ and $90°$, anisotropy does not significantly change the bounds on ξ, which remain close to $\pm 90°$. As is the case for isotropic media, when the angle ξ approaches the forbidden directions, the group attenuation coefficient $\mathcal{A}_g$ rapidly increases with $|\xi|$ and reaches values approximately twice as large as $\mathcal{A}|_{\xi=0°}$ (Figure 11).

For oblique propagation angles, α does not vanish, and the bounds on ξ become asymmetric with respect to $\xi = 0°$. This asymmetry is controlled by velocity-anisotropy coefficient γ and reaches its maximum for the phase angle $\theta = 45°$ (equation 39). The model in Figure 12a, taken from Carcione and Cavallini (1995), has an uncommonly large parameter γ equal to unity, and for $\theta = 45°$, the inhomogeneity angle can vary only between $-64°$ and $116°$. Therefore, strong velocity anisotropy might result in forbidden directions for angles $|\xi|$ much smaller than $90°$.

Still, the range of possible inhomogeneity angles (2β) remains close to $180°$ because the parameter $\beta \approx 90°$ (Figure 12a). For more-common, smaller values of parameter γ, the bounds on ξ become more symmetric with respect to $\xi = 0°$ and do not differ significantly from $\pm 90°$ (Figure 12b). The behavior of the coefficient $\mathcal{A}_g$ for large angles ξ in Figure 12 is similar to that in isotropic media.

DISCUSSION

Our analytic and numerical results prove that the normalized group attenuation coefficient $\mathcal{A}_g$ measured from seismic data is practically independent of the inhomogeneity angle (except for angles ξ approaching the forbidden directions) and

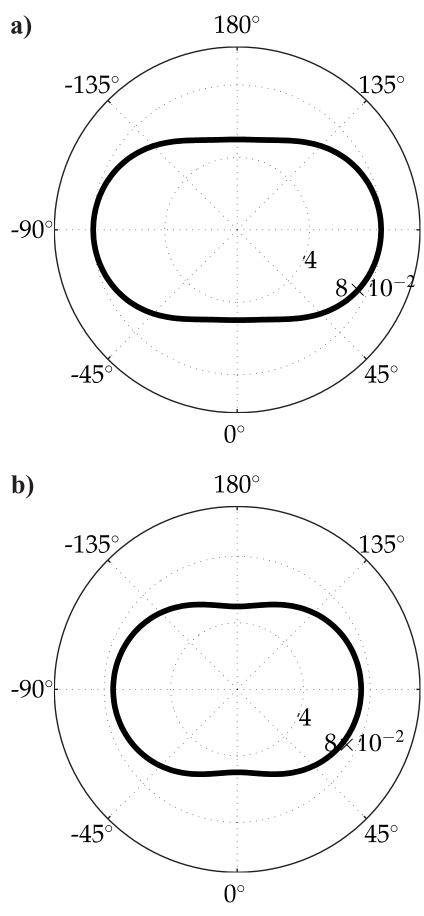

Figure 7. Exact (a) P-wave and (b) SH-wave coefficients $\mathcal{A}|_{\xi=0°}$ (gray curves) and $\mathcal{A}_g$ (black curves) in TI media as a function of the phase angle for $\xi = 0°$. Because $\mathcal{A}_g = \mathcal{A}|_{\xi=0°}$, the gray curves practically coincide with the black curves. The model parameters are given in Table 1.

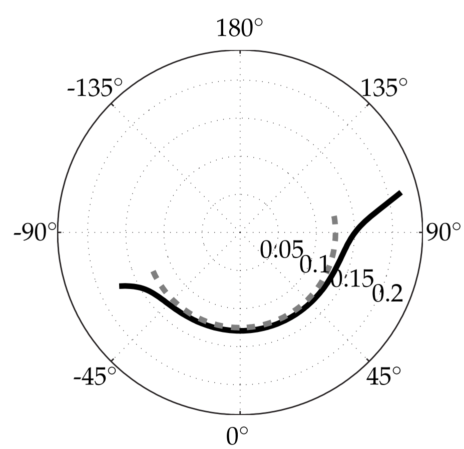

Figure 8. Exact P-wave group attenuation coefficient $\mathcal{A}_{g,P}$ (solid line) and approximate $\mathcal{A}_{g,P}$ from equation 34 (dashed line) in TI media for $\theta = 45°$ as a function of the angle ξ (numbers on the perimeter). The model parameters are given in Table 1.

is close to the normalized phase attenuation coefficient $\mathcal{A}|_{\xi=0^\circ}$. Behura and Tsvankin (2008) corroborate this conclusion by applying attenuation layer stripping and the spectral-ratio method to full-waveform P-wave synthetic data generated by a point source in layered anisotropic models. The interval coefficients $\mathcal{A}_g$ and $\mathcal{A}|_{\xi=0^\circ}$ estimated by Behura and Tsvankin (2008) from reflection amplitudes practically coincide, even at large offsets where the inhomogeneity angle reaches 45°.

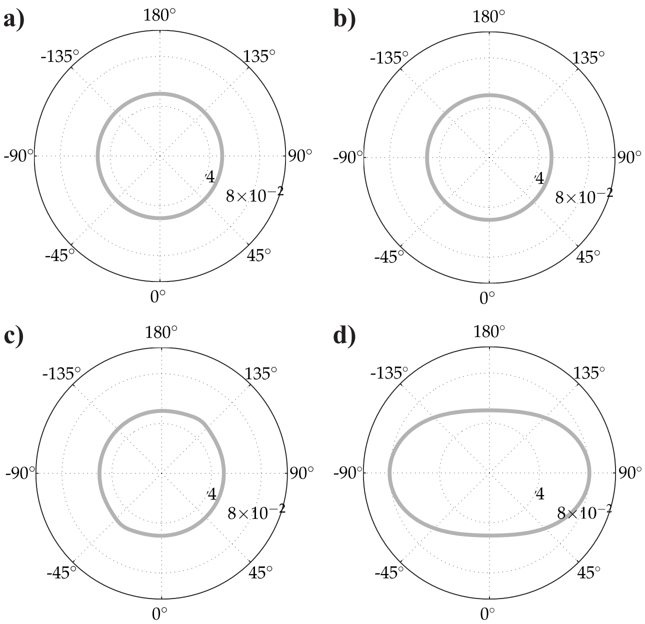

Figure 9. Exact P-wave group attenuation coefficient $\mathcal{A}_g$ for $\xi=60^\circ$ in (a) isotropic and (b), (c), and (d) TI media. In (b) and (c) only velocity varies with angle, whereas attenuation is isotropic; in (d) attenuation varies with angle, and velocity is isotropic. The model parameters are given in Table 1.

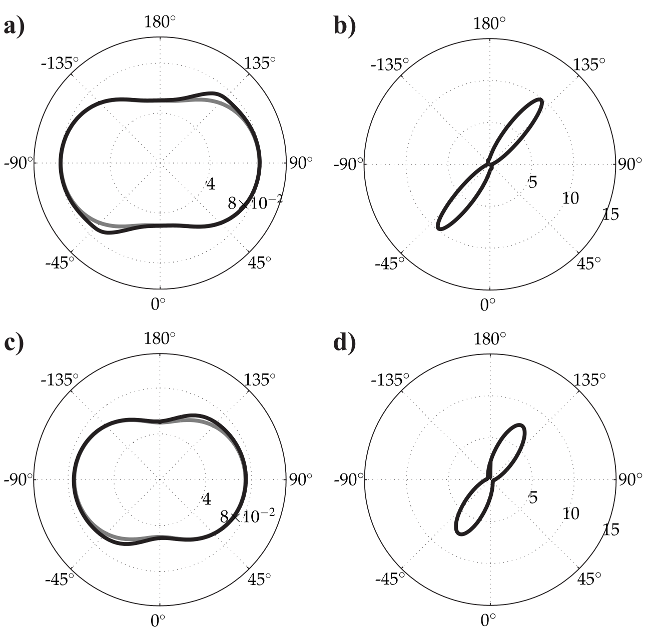

Figure 10. Exact (a) P-wave and (c) SH-wave coefficients $\mathcal{A}|_{\xi=0^\circ}$ (gray curve) and $\mathcal{A}_g$ (black curve) and (b) and (d) the percentage difference $|\mathcal{A}_g - \mathcal{A}|_{\xi=0^\circ}|$ in TI media as a function of the phase angle θ for $\xi=60^\circ$. The model parameters are listed in Table 1.

The coefficient $\mathcal{A}|_{\xi=0^\circ}$ in TI and orthorhombic media can be inverted for Thomsen-style attenuation-anisotropy parameters using the formalism developed by Zhu and Tsvankin (2006, 2007). Note that estimation of attenuation-anisotropy parameters from $\mathcal{A}|_{\xi=0^\circ}$ requires computation of the corresponding phase angle, which depends on the anisotropic velocity field. Even in strongly anisotropic models, however, the influence of attenuation on velocity is of the second order (see above), which implies that velocity analysis can be performed using existing methods. Then the reconstructed velocity field can be employed to recompute the known group direction into the phase direction needed in the inversion for attenuation-anisotropy parameters. Furthermore, given the large uncertainty of amplitude measurements, the difference between the phase and group directions for moderately anisotropic models should not substantially distort the results of attenuation analysis.

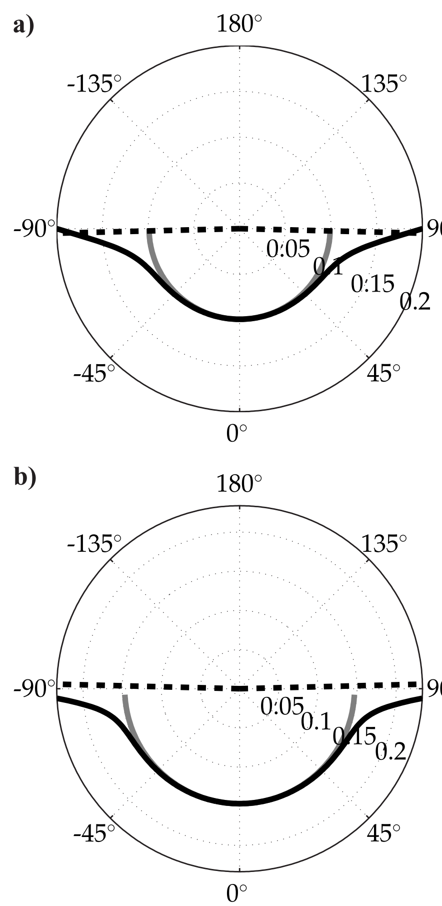

Figure 11. Exact SH-wave coefficients $\mathcal{A}|_{\xi=0^\circ}$ (gray curve) and $\mathcal{A}_g$ (black curve) in TI media for propagation in the directions (a) $\theta=0^\circ$ and (b) $\theta=90^\circ$, plotted as a function of the inhomogeneity angle ξ (numbers on the perimeter). The black dashed line marks the bounds of ξ computed from equations 38–40. The model parameters are listed in Table 1.

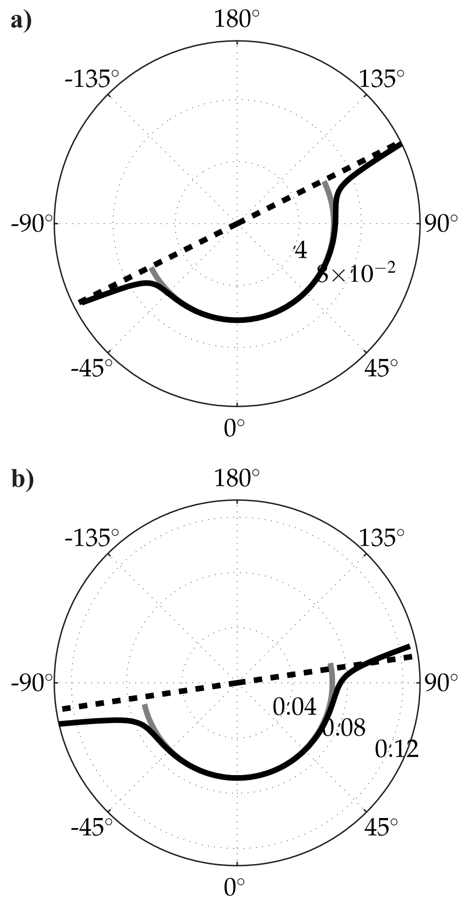

Figure 12. Exact SH-wave coefficients $\mathcal{A}|_{\xi=0^\circ}$ (gray curve) and $\mathcal{A}_g$ (black) as a function of ξ (numbers on the perimeter) for $\theta = 45^\circ$, $\gamma_Q = -0.5$ and (a) $\gamma = 1.0$; and (b) $\gamma = 0.3$. The black dashed line marks the bounds of ξ computed from equations 38–40. The model parameters are listed in Table 1.

CONCLUSIONS

We applied first-order perturbation theory to study the influence of the inhomogeneity angle on velocity and attenuation in arbitrarily anisotropic media. By adopting an attenuative, isotropic background medium, we were able to specify a background wave vector with an arbitrary inhomogeneity angle ξ. Perturbation analysis yields concise analytic expressions for the complex wave vector $\mathbf{k}$, the phase attenuation coefficient $\mathcal{A}|_{\xi=0^\circ}$, and the group attenuation coefficient $\mathcal{A}_g$ in terms of perturbations of the complex stiffness coefficients. To gain physical insight into the influence of the inhomogeneity angle, we also derived closed-form expressions for TI media by linearizing the general solutions in dimensionless velocity- and attenuation-anisotropy parameters.

For a wide range of small and moderate angles ξ, the phase-velocity function is practically independent of attenuation, while the group attenuation coefficient $\mathcal{A}_g$, which is measured from seismic data, is insensitive to the inhomogeneity angle. Furthermore, $\mathcal{A}_g$ practically coincides with the phase attenuation coefficient $\mathcal{A}|_{\xi=0^\circ}$, which is proportional to the angle-dependent inverse quality factor in anisotropic media. This conclusion remains valid even for uncommonly high attenuation ($Q \approx 10$) and strong velocity and attenuation anisotropy. The negligible difference between $\mathcal{A}_g$ and $\mathcal{A}|_{\xi=0^\circ}$ suggests that seismic data can be inverted for the attenuation-anisotropy parameters without knowledge of the inhomogeneity angle.

However, for larger angles ξ approaching the forbidden directions (i.e., the directions of the attenuation vector $\mathbf{k}^I$ for which solutions of the wave equation do not exist) the inhomogeneity angle has a strong influence on both attenuation and phase velocity. Whereas for isotropic media the inhomogeneity angle can vary between -90° and 90°, velocity anisotropy makes the bounds on the inhomogeneity angle asymmetric with respect to $\xi = 0^\circ$. In the vicinity of the forbidden directions, the coefficient $\mathcal{A}_g$ rapidly increases with $|\xi|$ and reaches values approximately twice as large as $\mathcal{A}|_{\xi=0^\circ}$. The range of such anomalous inhomogeneity angles, where $\mathcal{A}_g$ no longer represents a direct measure of the intrinsic attenuation, becomes wider for highly attenuative models.

ACKNOWLEDGMENTS

We are grateful to the members of the A(nisotropy)-Team of the Center for Wave Phenomena (CWP), Colorado School of Mines, for helpful discussions. The reviews by Ken Larner (associate editor) and referees of GEOPHYSICS helped to improve the paper. Support for this work was provided by the Consortium Project on Seismic Inverse Methods for Complex Structures at CWP and by the Petroleum Research Fund of the American Chemical Society.

APPENDIX A

COMPLEX WAVE VECTOR FOR ISOTROPIC ATTENUATIVE MEDIA

We consider a harmonic plane wave with an arbitrary inhomogeneity angle ξ propagating in isotropic attenuative media:

$$A(\mathbf{x},t) = A_0 e^{i(\omega t - \mathbf{k}\cdot\mathbf{x})}, \tag{A-1}$$

where ω is the angular frequency and $\mathbf{k} = \mathbf{k}^R - i\mathbf{k}^I$ is the complex wave vector responsible for the velocity and the attenuation coefficient. Substitution of the plane wave A-1 into the acoustic wave equation results in

$$k_1^2 + k_2^2 + k_3^2 = \frac{\omega^2}{V^2\left(1 + \dfrac{i}{Q}\right)}, \tag{A-2}$$

where V is the real part of the medium velocity, and Q is the quality factor. Dropping quadratic and higher-order terms in $1/Q$, we rewrite equation A-2 as

$$(k^R)^2 - 2i\,\mathbf{k}^R\cdot\mathbf{k}^I - (k^I)^2 = \frac{\omega^2}{V^2}\left(1 - \frac{i}{Q}\right); \tag{A-3}$$

$k^R = |\mathbf{k}^R|$ and $k^I = |\mathbf{k}^I|$. Equation A-3 can be separated into the real and imaginary parts:

$$(k^R)^2 - (k^I)^2 = \frac{\omega^2}{V^2}, \tag{A-4}$$

and

$$\mathbf{k}^R\cdot\mathbf{k}^I = \frac{\omega^2}{2V^2Q}. \tag{A-5}$$

When the medium is nonattenuative and $1/Q = 0$, the right side of equation A-5 vanishes. Then, the vectors $\mathbf{k}^R$ and $\mathbf{k}^I$ of an inhomogeneous (evanescent) plane wave have to be orthogonal, with the relationship between k^R and k^I determined by equation A-4.

Because the factor Q responsible for attenuation is positive, equation A-5 can be satisfied only if $\mathbf{k}^R \cdot \mathbf{k}^I > 0$, which requires that $\cos\xi > 0$ and $\xi < 90°$. (We make the assumption that $\xi > 0$ because the solutions of equations A-4 and A-5 do not depend on the sign of ξ.) With the inhomogeneity angle smaller than 90°, equation A-5 allows us to express k^I through k^R as

$$k^I = \frac{\omega^2}{2k^R V^2 Q \cos\xi}. \tag{A-6}$$

Substitution of k^I into equation A-4 yields a quadratic equation for $(k^R)^2$, which has only one positive solution:

$$(k^R)^2 = \frac{\omega^2}{2V^2}\left[\sqrt{1 + \frac{1}{(Q\cos\xi)^2}} + 1\right]. \tag{A-7}$$

The corresponding imaginary part k^I can be obtained from either equation A-4 or A-6:

$$(k^I)^2 = \frac{\omega^2}{2V^2}\left[\sqrt{1 + \frac{1}{(Q\cos\xi)^2}} - 1\right]. \tag{A-8}$$

For typical large values of the quality factor, the product $(Q\cos\xi) \gg 1$, unless the inhomogeneity angle is close to 90°. Expanding the radical in equations A-7 and A-8 in $1/(Q\cos\xi)^2$, we find

$$k^R \cong \frac{\omega}{V}\left[1 + \frac{1}{8(Q\cos\xi)^2}\right], \tag{A-9}$$

and

$$k^I \cong \frac{\omega}{2VQ\cos\xi}\left[1 - \frac{1}{8(Q\cos\xi)^2}\right]. \tag{A-10}$$

Equations A-9 and A-10 can be simplified further by neglecting the small (compared to unity) term $1/[8(Q\cos\xi)^2]$:

$$k^R = \frac{\omega}{V}, \tag{A-11}$$

$$k^I = \frac{\omega}{2VQ\cos\xi}. \tag{A-12}$$

Large inhomogeneity angles

Although equations A-11 and A-12 are sufficiently accurate for a wide range of inhomogeneity angles, they break down when $\xi \to 90°$. For $(Q\cos\xi) \ll 1$, equations A-7 and A-8 can be approximated by

$$k^R = \frac{\omega}{V\sqrt{2Q\cos\xi}}\left(1 + \frac{Q\cos\xi}{2}\right), \tag{A-13}$$

$$k^I = \frac{\omega}{V\sqrt{2Q\cos\xi}}\left(1 - \frac{Q\cos\xi}{2}\right). \tag{A-14}$$

The phase attenuation coefficient $\mathcal{A}$ can be found from equations A-13 and A-14:

$$\mathcal{A} = \frac{k^I}{k^R} = 1 - Q\cos\xi; \tag{A-15}$$

here, we have dropped the term quadratic in $(Q\cos\xi)$.

Group angle

In elastic isotropic media, the group- and phase-velocity vectors are always parallel. However, if the medium is strongly attenuative and $\xi \neq 0°$, the group direction might deviate from the phase direction. The group-velocity vector in arbitrarily anisotropic, attenuative media can be computed from (Červený and Pšenčík, 2006)

$$(V_g)_i = \frac{S_i}{\mathbf{S}\cdot\mathbf{p}^R} = \frac{(a_{ijkl}\, g_k g_j^* p_l)^R}{(a_{ijkl}\, g_k g_i^* p_l)^R p_j^R}, \tag{A-16}$$

where $\mathbf{S}$ is the energy flux, a_{ijkl} is the density-normalized stiffness tensor, $\mathbf{p}$ is the slowness vector, and $\mathbf{g}$ is the polarization vector. The superscripts R and $*$ represent the real part and complex conjugate, respectively.

For isotropic media, equation A-16 yields the following components of $\mathbf{V}_g$:

$$\mathbf{V}_g = \frac{\omega}{k^R}\left[\frac{k^I \sin\xi}{k^R Q + k^I \cos\xi},\ 0,\ 1\right]. \tag{A-17}$$

From equation A-17, we find the group angle ψ:

$$\tan\psi = \frac{k^I \sin\xi}{k^R Q + k^I \cos\xi}. \tag{A-18}$$

To obtain the group angle for small and moderate inhomogeneity angles, we substitute equations A-11 and A-12 into equation A-18, yielding

$$\tan\psi = \frac{\tan\xi}{1 + 2Q^2} \ll 1. \tag{A-19}$$

For angles ξ approaching 90°, we substitute equation A-15 into equation A-18 and linearize the result in $\cos\xi$ to get

$$\tan\psi = \frac{1}{Q} - \cos\xi. \tag{A-20}$$

It is clear that for large inhomogeneity angles and strongly attenuative media, angle ψ might not be negligible.

APPENDIX B

PERTURBATION ANALYSIS

Here, we derive analytic expressions for the real and imaginary parts of the wave vector in arbitrarily anisotropic, attenuative media using first-order perturbation theory. A homogeneous, isotropic, attenuative full space is taken as the background medium (Figure B-1a). The inhomogeneity angle ξ between the real $(k^{R,0})$ and imaginary $(k^{I,0})$ parts of the wave vector in the background can be arbitrarily large. The background medium is perturbed to make it anisotropic in terms of both velocity and attenuation (Figure B-1b), which results in perturbations of the real (Δk^R) and imaginary (Δk^I) parts of the wave vector. Because the inhomogeneity angle ξ is a free parameter, we choose not to perturb it when making the medium anisotropic. This implies that the vectors $\mathbf{k}^R$ and $\mathbf{k}^{R,0}$, as well as $\mathbf{k}^I$ and $\mathbf{k}^{I,0}$, are parallel.

We choose $\mathbf{k}^0$ such that $\mathbf{k}^{R,0}$ coincides with the axis x_3 and $\mathbf{k}^{I,0}$ lies in the $[x_1,x_3]$-plane (Figure B-1a and B-1b). This approach differs from the one adopted by Jech and Pšenčík (1989), Červený and Pšenčík (2008b), and Vavryčuk (2008), who used a fixed reference frame. To compute perturbations for a different vector $\mathbf{k}$ in the same medium, we rotate the coordinate frame such that $\mathbf{k}^R$ coincides with the axis x_3 and $\mathbf{k}^I$ lies in the $[x_1,x_3]$-plane. This approach involves the rotation of the density-normalized stiffness tensor a_{ijkl} but obviates the need to introduce two additional angles needed to define the orientations of $\mathbf{k}^R$ and $\mathbf{k}^I$.

Real and imaginary parts of the wave vector

We start with the Christoffel equation in the perturbed medium:

$$(G_{ik} - \delta_{ik}) g_k = 0, \tag{B-1}$$

where $G_{ik} = a_{ijkl} p_j p_l$ is the Christoffel matrix, $\mathbf{p}$ is the complex slowness vector, and $\mathbf{g}$ is the polarization vector of the plane wave. Perturbation of equation B-1 yields

$$(G^0_{ik} + \Delta G_{ik} - \delta_{ik})(g^0_k + \Delta g_k) = 0, \tag{B-2}$$

which can be linearized to obtain

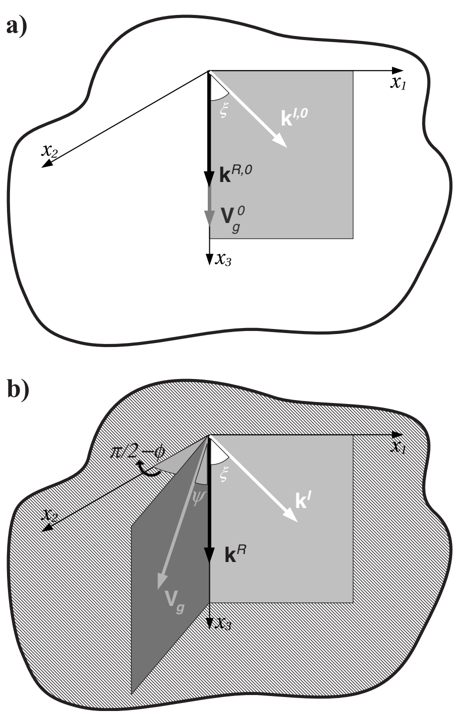

Figure B-1. (a) Isotropic attenuative background medium is perturbed to make it (b) anisotropic. The real and imaginary parts of the wave vector in the background are $\mathbf{k}^{R,0}$ and $\mathbf{k}^{I,0}$, and $\mathbf{k}^R = \mathbf{k}^{R,0} + \Delta\mathbf{k}^R$ and $\mathbf{k}^I = \mathbf{k}^{I,0} + \Delta\mathbf{k}^I$ form the wave vector in the perturbed medium; ξ is the inhomogeneity angle. The vectors $\mathbf{k}^{R,0}$ and $\mathbf{k}^R$ are parallel to the vertical x_3-direction, and $\mathbf{k}^{I,0}$ and $\mathbf{k}^I$ are confined to the $[x_1,x_3]$-plane. $\mathbf{V}_g^0$ is the group velocity in the background; ψ is the polar group angle after the perturbation, and ϕ is the azimuth of the perturbed vector $\mathbf{V}_g$ with respect to the $[x_1,x_3]$-plane.

$$(G^0_{ik} - \delta_{ik})\Delta g_k + \Delta G_{ik} g^0_k = 0, \tag{B-3}$$

where $\mathbf{g}^0$ is the plane-wave polarization in the background and $\Delta\mathbf{g}$ is the perturbation of the polarization vector. The polarization $\mathbf{g}^0$ defines whether the wave mode is P, SV, or SH. The mode obtained by perturbing the SV-wave will be denoted S_1, and the perturbed SH-wave will be denoted S_2. Multiplying equation B-3 with g^0_i (Jech and Pšenčík, 1989) reduces equation B-3 to

$$\Delta G_{ik} g^0_i g^0_k = 0, \tag{B-4}$$

with

$$\Delta G_{ik} = \Delta a_{ijkl} p^0_j p^0_l + 2 a^0_{ijkl} \Delta p_j p^0_l, \tag{B-5}$$

where a^0_{ijkl} and $\mathbf{p}^0$ are defined in the isotropic background, and Δa_{ijkl} and $\Delta\mathbf{p}$ are the perturbations. The tensors a^0_{ijkl} and Δa_{ijkl} are given by

$$a^0_{ijkl} = a^{R,0}_{ijkl} + i a^{I,0}_{ijkl} = a^{R,0}_{ijkl}\left(1 + \frac{i}{Q^0_{ijkl}}\right), \tag{B-6}$$

$$\Delta a_{ijkl} = \Delta a^R_{ijkl} + i \Delta a^I_{ijkl}, \tag{B-7}$$

where the superscripts R and I denote the real and imaginary parts, and Q^0_{ijkl} is the ratio $a^{R,0}_{ijkl}/a^{I,0}_{ijkl}$. The background slowness $\mathbf{p}^0$ and its perturbation $\Delta\mathbf{p}$ can be expressed as

$$\mathbf{p}^0 = [-ip^{I,0}\sin\xi,\ 0,\ p^{R,0} - ip^{I,0}\cos\xi], \tag{B-8}$$

$$\Delta\mathbf{p} = [-i\Delta p^I\sin\xi,\ 0,\ \Delta p^R - i\Delta p^I\cos\xi], \tag{B-9}$$

where $p^{R,0}$, $p^{I,0}$ and Δp^R, Δp^I are the magnitudes of the real and imaginary parts of $\mathbf{p}^0$ and $\Delta\mathbf{p}$, respectively.

Assuming $(Q^0\cos\xi) \gg 1$, we solve equation B-4 for $\Delta k^R = \omega\Delta p^R$ and $\Delta k^I = \omega\Delta p^I$:

$$\frac{\Delta k^R}{k^{R,0}} = -\frac{\chi^R}{2} - \frac{\chi^I}{2Q^0}\left(1 - \frac{\sec^2\xi}{2}\right), \tag{B-10}$$

$$\frac{\Delta k^I}{k^{I,0}} = -\frac{\chi^R}{2} + Q^0\chi^I, \tag{B-11}$$

where χ^R and χ^I are the real and imaginary parts of $\chi = \Delta a_{ijkl} p^0_j p^0_l g^0_i g^0_k$. The above analysis is valid for all three modes (P-, S_1-, and S_2-waves). By choosing the corresponding $\mathbf{k}^0$ and χ, we can compute the perturbations of the complex wave vector for any of the three modes. The term χ for P-, S_1-, and S_2-waves has the form

$$\chi_P = \frac{1}{V^2_{P0}}\left(\Delta a^R_{33} + \frac{\Delta a^I_{33}}{Q_{P0}} + \frac{2\Delta a^I_{35}}{Q_{P0}}\tan\xi\right) + i\frac{1}{V^2_{P0}}\left(-\frac{\Delta a^R_{33}}{Q_{P0}} + \Delta a^I_{33} - \frac{2\Delta a^R_{35}}{Q_{P0}}\tan\xi\right), \tag{B-12}$$

$$\chi_{S_1} = \frac{1}{V^2_{S0}}\left(\Delta a^R_{55} + \frac{\Delta a^I_{55}}{Q_{S0}} + \frac{\Delta a^I_{15} - \Delta a^I_{35}}{Q_{S0}}\tan\xi\right)$$

$$+ i \frac{1}{V_{S0}^2}\left(-\frac{\Delta a_{55}^R}{Q_{S0}} + \Delta a_{55}^I - \frac{\Delta a_{15}^R - \Delta a_{35}^R}{Q_{S0}} \tan \xi \right), \quad \text{(B-13)}$$

and

$$\chi_{S_2} = \frac{1}{V_{S0}^2}\left(\Delta a_{44}^R + \frac{\Delta a_{44}^I}{Q_{S0}} + \frac{\Delta a_{46}^I}{Q_{S0}} \tan \xi \right) + i \frac{1}{V_{S0}^2}\left(-\frac{\Delta a_{44}^R}{Q_{S0}} + \Delta a_{44}^I - \frac{\Delta a_{46}^R}{Q_{S0}} \tan \xi \right); \quad \text{(B-14)}$$

Q_{P0} and Q_{S0} are the P- and S-wave quality factors in the background medium. Substituting equations B-12–B-14 into equations B-10 and B-11 and retaining only the terms linear in Δa_{ij} yields

$$\frac{\Delta k_P^R}{k_P^{R,0}} \approx -\frac{1}{V_{P0}^2}\left[\frac{\Delta a_{33}^R}{2} + \frac{\Delta a_{33}^I}{Q_{P0}}\left(1 - \frac{\sec^2 \xi}{4}\right) + \frac{\Delta a_{35}^I}{Q_{P0}} \tan \xi \right], \quad \text{(B-15)}$$

$$\frac{\Delta k_P^I}{k_P^{I,0}} \approx -\frac{1}{V_{P0}^2}\left(\frac{3\Delta a_{33}^R}{2} - Q_{P0}\Delta a_{33}^I + 2\Delta a_{35}^R \tan \xi \right), \quad \text{(B-16)}$$

$$\frac{\Delta k_{S_1}^R}{k_{S_1}^{R,0}} \approx -\frac{1}{V_{S0}^2}\left[\frac{\Delta a_{55}^R}{2} + \frac{\Delta a_{55}^I}{Q_{S0}}\left(1 - \frac{\sec^2 \xi}{4}\right) + \frac{\Delta a_{15}^I - \Delta a_{35}^I}{2Q_{S0}} \tan \xi \right], \quad \text{(B-17)}$$

$$\frac{\Delta k_{S_1}^I}{k_{S_1}^{I,0}} \approx -\frac{1}{V_{S0}^2}\left(\frac{3\Delta a_{55}^R}{2} - Q_{S0}\Delta a_{55}^I + (\Delta a_{15}^R - \Delta a_{35}^R) \tan \xi \right), \quad \text{(B-18)}$$

$$\frac{\Delta k_{S_2}^R}{k_{S_2}^{R,0}} \approx -\frac{1}{V_{S0}^2}\left[\frac{\Delta a_{44}^R}{2} + \frac{\Delta a_{44}^I}{Q_{S0}}\left(1 - \frac{\sec^2 \xi}{4}\right) + \frac{\Delta a_{46}^I}{2Q_{S0}} \tan \xi \right], \quad \text{(B-19)}$$

and

$$\frac{\Delta k_{S_2}^I}{k_{S_2}^{I,0}} \approx -\frac{1}{V_{S0}^2}\left(\frac{3\Delta a_{44}^R}{2} - Q_{S0}\Delta a_{44}^I + \Delta a_{46}^R \tan \xi \right). \quad \text{(B-20)}$$

Normalized phase attenuation coefficient

We linearize the normalized phase attenuation coefficient $\mathcal{A}$ for $\xi = 0°$ by retaining only the first-order terms:

$$\mathcal{A}|_{\xi=0°} = \left.\frac{k^I}{k^R}\right|_{\xi=0°} = \left.\frac{k^{I,0} + \Delta k^I}{k^{R,0} + \Delta k^R}\right|_{\xi=0°} \quad \text{(B-21)}$$

$$= \frac{1}{2Q_0}\left(1 + \frac{\Delta k^I}{k^{I,0}} - \frac{\Delta k^R}{k^{R,0}}\right). \quad \text{(B-22)}$$

By substituting Δk^R and Δk^I from equations B-15–B-20 into equation B-22, we obtain $\mathcal{A}|_{\xi=0°}$ in arbitrarily anisotropic media for all three modes:

$$\mathcal{A}|_{\xi=0°,P} = \frac{1}{2Q_{P0}} - \frac{1}{2V_{P0}^2}\left(\frac{\Delta a_{33}^R}{Q_{P0}} - \Delta a_{33}^I \right), \quad \text{(B-23)}$$

$$\mathcal{A}|_{\xi=0°,S_1} = \frac{1}{2Q_{S0}} - \frac{1}{2V_{S0}^2}\left(\frac{\Delta a_{55}^R}{Q_{S0}} - \Delta a_{55}^I \right), \quad \text{(B-24)}$$

$$\mathcal{A}|_{\xi=0°,S_2} = \frac{1}{2Q_{S0}} - \frac{1}{2V_{S0}^2}\left(\frac{\Delta a_{44}^R}{Q_{S0}} - \Delta a_{44}^I \right). \quad \text{(B-25)}$$

Normalized group attenuation coefficient

To obtain the normalized group attenuation from equation 32, we find the product $(\tan \psi \cos \phi) = V_{g1}/V_{g3}$ from equation A-16:

$$\tan \psi_P \cos \phi_P = \frac{2\Delta a_{35}^R}{V_{P0}^2}, \quad \text{(B-26)}$$

$$\tan \psi_{S_1} \cos \phi_{S_1} = \frac{\Delta a_{15}^R - \Delta a_{35}^R}{V_{S0}^2}, \quad \text{(B-27)}$$

and

$$\tan \psi_{S_2} \cos \phi_{S_2} = \frac{\Delta a_{46}^R}{V_{S0}^2}, \quad \text{(B-28)}$$

where only the leading-order terms are retained.

Next, we substitute Δk^R and Δk^I from equations B-15–B-20 and $\tan \psi$ from equations B-26–B-28 into equation 32 and retain only the terms linear in Δa_{ij}:

$$\mathcal{A}_{g,P} = \frac{1}{2Q_{P0}} - \frac{1}{2V_{P0}^2}\left(\frac{\Delta a_{33}^R}{Q_{P0}} - \Delta a_{33}^I \right), \quad \text{(B-29)}$$

$$\mathcal{A}_{g,S_1} = \frac{1}{2Q_{S0}} - \frac{1}{2V_{S0}^2}\left(\frac{\Delta a_{55}^R}{Q_{S0}} - \Delta a_{55}^I \right), \quad \text{(B-30)}$$

and

$$\mathcal{A}_{g,S_2} = \frac{1}{2Q_{S0}} - \frac{1}{2V_{S0}^2}\left(\frac{\Delta a_{44}^R}{Q_{S0}} - \Delta a_{44}^I \right). \quad \text{(B-31)}$$

APPENDIX C

SHEAR-WAVE PHASE AND GROUP QUANTITIES IN TI MEDIA

Here, we present closed-form expressions for the shear-wave parameters Δk^R, Δk^I, $\mathcal{A}$, and $\mathcal{A}_g$ in TI media. Note that all equations in

Appendix A are derived for the coordinate frame defined by the vectors $\mathbf{k}^R$ and $\mathbf{k}^I$. Therefore, in order to obtain Δk^R, Δk^I, $\mathcal{A}$, and $\mathcal{A}_g$ as a function of the phase angle θ (the angle between $\mathbf{k}^R$ and the x_3-axis), one needs to rotate tensor Δa_{ijkl} accordingly. Because $\mathbf{k}^I$ is assumed to lie in the plane defined by $\mathbf{k}^R$, Δa_{ijkl} in Appendix A is rotated by the phase angle θ around the x_2-axis.

By linearizing the rotated tensor Δa_{ijkl} in the velocity-anisotropy parameters ε, δ, and γ and in the attenuation-anisotropy parameters ε_Q, δ_Q, and γ_Q (Zhu and Tsvankin, 2006), we obtain the real ($\mathbf{k}^R$) and imaginary ($\mathbf{k}^I$) parts of the wave vector from equations B-17–B-20:

$$\frac{\Delta k^R_{\mathrm{SV}}}{k^{R,0}_{\mathrm{SV}}} = -\,\sigma \sin^2\theta \cos^2\theta, \qquad \text{(C-1)}$$

$$\frac{\Delta k^I_{\mathrm{SV}}}{k^{I,0}_{\mathrm{SV}}} = (\varepsilon_Q - \delta_Q)\frac{\mathsf{g}^2}{\mathsf{g}_Q}\sin^2\theta\cos^2\theta + \sigma\frac{2-3\mathsf{g}_Q}{\mathsf{g}_Q}\sin^2\theta\cos^2\theta - \sigma\sin 2\theta\cos 2\theta\tan\xi, \qquad \text{(C-2)}$$

$$\frac{\Delta k^R_{\mathrm{SH}}}{k^{R,0}_{\mathrm{SH}}} = -\,\gamma\sin^2\theta, \qquad \text{(C-3)}$$

and

$$\frac{\Delta k^I_{\mathrm{SH}}}{k^{I,0}_{\mathrm{SH}}} = \gamma_Q\sin^2\theta - \gamma\sin^2\theta - \gamma\sin 2\theta\tan\xi, \qquad \text{(C-4)}$$

where $\mathsf{g} = V_{\mathrm{P0}}/V_{\mathrm{S0}}$, the parameter $\sigma = \mathsf{g}^2(\varepsilon - \delta)$ controls the SV-wave phase velocity, $\mathsf{g}_Q = Q_{\mathrm{P0}}/Q_{\mathrm{S0}}$, and the parameters γ and γ_Q are responsible for the SH-wave velocity and attenuation anisotropy, respectively (Zhu and Tsvankin, 2006).

The normalized SV- and SH-wave phase attenuation coefficients for $\xi = 0°$ can be found from equations B-24 and B-25:

$$\mathcal{A}|_{\xi=0°,\,\mathrm{SV}} = \frac{1}{2Q_{\mathrm{S0}}}(1 + \sigma_Q\sin^2\theta\cos^2\theta), \qquad \text{(C-5)}$$

and

$$\mathcal{A}|_{\xi=0°,\,\mathrm{SH}} = \frac{1}{2Q_{\mathrm{S0}}}(1 + \gamma_Q\sin^2\theta), \qquad \text{(C-6)}$$

where the parameter σ_Q (Zhu and Tsvankin, 2006) controls the SV-wave attenuation coefficient:

$$\sigma_Q = \frac{1}{\mathsf{g}_Q}[2\sigma(1-\mathsf{g}_Q) + \mathsf{g}^2(\varepsilon_Q - \delta_Q)]. \qquad \text{(C-7)}$$

To obtain the linearized shear-wave group angles in TI media, we use equations B-27 and B-28 (see also Tsvankin, 2005):

$$\tan\psi_{\mathrm{SV}}\cos\phi_{\mathrm{SV}} = \sigma\sin 2\theta\cos 2\theta \qquad \text{(C-8)}$$

and

$$\tan\psi_{\mathrm{SH}}\cos\phi_{\mathrm{SH}} = \gamma\sin 2\theta. \qquad \text{(C-9)}$$

Substituting the anisotropy parameters into equations B-30 and B-31 yields the following group attenuation coefficients:

$$\mathcal{A}_{\mathrm{g,\,SV}} = \frac{1}{2Q_{\mathrm{S0}}}(1 + \sigma_Q\sin^2\theta\cos^2\theta), \qquad \text{(C-10)}$$

and

$$\mathcal{A}_{\mathrm{g,\,SH}} = \frac{1}{2Q_{S0}}(1 + \gamma_Q\sin^2\theta). \qquad \text{(C-11)}$$

APPENDIX D

ATTENUATION FOR LARGE INHOMOGENEITY ANGLES

Here we develop closed-form expressions for the wave vector $\mathbf{k}$ and group attenuation coefficient $\mathcal{A}_g$ for large angles ξ. For simplicity, we analyze only S_2-waves; expressions for P- and S_1-waves can be derived using the same procedure. The development follows the approach described in Appendix B. However, the group angle ψ^0 in the background does not vanish (equation 26), and the background vector $\mathbf{k}^0 = \mathbf{k}^{R,0} - i\mathbf{k}^{I,0}$ is given by equations 23 and 24. (Note that for small and moderate angles ξ considered in Appendix B, the group angle ψ^0 was zero.) For large ξ, the real ($k^{R,0}$) and imaginary ($k^{I,0}$) parts of the background wave vector are related by (equation 25)

$$\frac{k^{I,0}}{k^{R,0}} = 1 - Q^0\cos\xi, \qquad \text{(D-1)}$$

and the group angle ψ^0 is expressed as (equation 26)

$$\tan\psi^0 = \frac{1}{Q^0} - \cos\xi, \qquad \text{(D-2)}$$

where Q^0 is the background quality factor. Perturbation produces a change in both the wave vector ($\Delta k^R - i\Delta k^I$) and the group direction.

First, we obtain k^R and k^I by solving equation B-4 and linearizing the result in Δa_{ij}. Eliminating terms quadratic or higher-order in ($Q^0\cos\xi$) and those proportional to ($\Delta a_{ij}Q^0\cos\xi$), as well as setting terms quadratic in $\sin\xi$ to unity, we find

$$\frac{k^R_{\mathrm{S}_2}}{k^{R,0}_{\mathrm{S}_2}} = \frac{k^I_{\mathrm{S}_2}}{k^{I,0}_{\mathrm{S}_2}} = 1 - \frac{1}{2V^2_{\mathrm{S0}}}\left(\Delta a^R_{46} + \frac{\Delta a^I_{46}}{Q_{\mathrm{S0}}}\right)\tan\xi + \frac{1}{4V^2_{\mathrm{S0}}\cos\xi}\left(\Delta a^I_{44} - \frac{\Delta a^R_{44}}{Q_{\mathrm{S0}}} - \Delta a^I_{66} + \frac{\Delta a^R_{66}}{Q_{\mathrm{S0}}}\right). \qquad \text{(D-3)}$$

For the special case of TI media, the S_2-mode becomes the SH-wave, and equation D-3 (after eliminating terms proportional to γ/Q^2_{S0} and $\gamma_Q/Q^2_{\mathrm{S0}}$) takes the form

$$\frac{k^R_{\mathrm{S}_2}}{k^{R,0}_{\mathrm{S}_2}} = \frac{k^I_{\mathrm{S}_2}}{k^{I,0}_{\mathrm{S}_2}} \approx 1 + \frac{\gamma\sin 2\theta}{2}\tan\xi - \frac{\gamma_Q\cos 2\theta}{4Q_{\mathrm{S0}}}\frac{1}{\cos\xi}. \qquad \text{(D-4)}$$

The product $\tan\psi\cos\phi$ needed to find $\mathcal{A}_g$ can be obtained from equation A-16:

$$\tan\psi\cos\phi = \frac{1}{Q_{S0}} - \cos\xi - \frac{1}{4V_{S0}^2}\left[\frac{2\Delta a_{46}^I}{Q_{S0}} - 6\Delta a_{46}^R + \left(\frac{3\Delta a_{44}^R}{Q_{S0}} + \frac{\Delta a_{66}^R}{Q_{S0}} + \Delta a_{44}^I - 5\Delta a_{66}^I\right)\sin\xi\right]. \quad \text{(D-5)}$$

The group attenuation coefficient $\mathcal{A}_g$ is found by substituting equations D-1–D-5 into equation 31:

$$\mathcal{A}_g = \frac{1}{Q_{S0}} - \cos\xi - \frac{1}{4V_{S0}^2}\left[\frac{3\Delta a_{44}^R}{Q_{S0}} + \frac{\Delta a_{66}^R}{Q_{S0}} + \Delta a_{44}^I - 5\Delta a_{66}^I + \left(\frac{2\Delta a_{46}^I}{Q_{S0}} - 6\Delta a_{46}^R\right)\sin\xi\right]; \quad \text{(D-6)}$$

equation D-6 is linearized in Δa_{ij} and $(Q_{S0}\cos\xi)$, and terms proportional to $(\Delta a_{ij} Q_{S0}\cos\xi)$ have been eliminated. The range of ξ for which equation D-6 is valid is set by the assumption $(Q_{S0}\cos\xi) \ll 1$, which ensures that $\mathcal{A}_g$ is positive. For the special case of TI media, $\mathcal{A}_g$ takes a simpler form after linearization in the anisotropy parameters:

$$\mathcal{A}_g = \frac{1}{Q_{S0}} - \cos\xi - \frac{3\gamma\sin 2\theta}{2}\sin\xi + \frac{2\gamma\cos 2\theta}{Q_{S0}} + \frac{\gamma_Q\cos 2\theta}{4Q_{S0}} + \frac{\gamma_Q\cos^2\theta}{4Q_{S0}}. \quad \text{(D-7)}$$

REFERENCES

Behura, J., and I. Tsvankin, 2008, Estimation of interval anisotropic attenuation from reflection data: 78th Annual International Meeting, SEG, Expanded Abstracts, 260.

Boulanger, P., and M. Hayes, 1993, Bivectors and waves in mechanics and optics: CRC Press.

Carcione, J. M., and F. Cavallini, 1995, Forbidden directions for inhomogeneous pure shear waves in dissipative anisotropic media: Geophysics, **60**, 522–530.

Červený, V., and I. Pšenčík, 2005a, Plane waves in viscoelastic anisotropic media — I. Theory: Geophysical Journal International, **161**, no. 1, 197–212.

———, 2005b, Plane waves in viscoelastic anisotropic media — II. Numerical examples: Geophysical Journal International, **161**, 213–229.

———, 2006, Energy flux in viscoelastic anisotropic media: Geophysical Journal International, **166**, 1299–1317.

———, 2008a, Quality factor Q in dissipative anisotropic media: Geophysics, **73**, no. 4, T63–T75.

———, 2008b, Weakly inhomogeneous plane waves in anisotropic, weakly dissipative media: Geophysical Journal International, **172**, 663–673.

Dasgupta, R., and R. A. Clark, 1998, Estimation of Q from surface seismic reflection data: Geophysics, **63**, 2120–2128.

Declercq, N. F., R. Briers, J. Degrieck, and O. Leroy, 2005, The history and properties of ultrasonic inhomogeneous waves: IEEE Transactions on Ultrasonics, Ferroelectrics and Frequency Control, **52**, 776–791.

Deschamps, M., and F. Assouline, 2000, Attenuation along the poynting vector direction of inhomogeneous plane waves in absorbing and anisotropic solids: Acustica, **86**, 295–302.

Gajewski, D., and I. Pšenčík, 1992, Vector wavefields for weakly attenuating anisotropic media by the ray method: Geophysics, **57**, 27–38.

Hauge, P. S., 1981, Measurements of attenuation from vertical seismic profiles: Geophysics, **46**, 1548–1558.

Huang, W., R. Briers, S. I. Rokhlin, and O. Leroy, 1994, Experimental study of inhomogeneous wave reflection from a solid-air periodically rough boundary using leaky rayleigh waves: The Journal of the Acoustical Society of America, **96**, 363–369.

Jech, J., and I. Pšenčík, 1989, First-order perturbation method for anisotropic media: Geophysical Journal International, **99**, 369–376.

Johnston, D. H., and M. N. Toksöz, 1981, Seismic wave attenuation: Society of Exploration Geophysicists.

Krebes, E. S., and L. H. T. Le, 1994, Inhomogeneous plane waves and cylindrical waves in anisotropic anelastic media: Journal of Geophysical Research, **99**, 899–919.

Tonn, R., 1991, The determination of the seismic quality factor Q from VSP data: A comparison of different computational methods: Geophysical Prospecting, **39**, 1–27.

Tsvankin, I., 1995, Seismic wavefields in layered isotropic media: Samizdat Press.

———, 2005, Seismic signatures and analysis of reflection data in anisotropic media, 2nd edition: Elsevier Science.

Vavryčuk, V., 2007, Ray velocity and ray attenuation in homogeneous anisotropic viscoelastic media: Geophysics, **72**, no. 6, D119–D127.

———, 2008, Velocity, attenuation, and quality factor in anisotropic viscoelastic media: A perturbation approach: Geophysics, **73**, no. 5, D63–D73.

Zhu, Y., 2006, Seismic wave propagation in attenuative anisotropic media: Ph.D. thesis, Colorado School of Mines.

Zhu, Y., and I. Tsvankin, 2006, Plane-wave propagation in attenuative transversely isotropic media: Geophysics, **71**, no 2, T17–T30.

———, 2007, Plane-wave attenuation anisotropy in orthorhombic media: Geophysics, **72**, no. 1, D9–D19.

Zhu, Y., I. Tsvankin, P. Dewangan, and K. van Wijk, 2007, Physical modeling and analysis of P-wave attenuation anisotropy in transversely isotropic media: Geophysics, **72**, no. 1, D1–D7.